

Ab Initio Description of the Exotic Unbound ${}^7\text{He}$ Nucleus

Simone Baroni,^{1,2,*} Petr Navrátil,^{2,3,†} and Sofia Quaglioni^{3,‡}

¹*Physique Nucléaire Théorique, Université Libre de Bruxelles, C.P. 229, B-1050 Bruxelles, Belgium*

²*TRIUMF, 4004 Wesbrook Mall, Vancouver, British Columbia V6T 2A3, Canada*

³*Lawrence Livermore National Laboratory, P. O. Box 808, L-414, Livermore, California 94551, USA*
(Received 8 October 2012; revised manuscript received 19 November 2012; published 11 January 2013)

The neutron-rich unbound ${}^7\text{He}$ nucleus has been the subject of many experimental investigations. While the ground-state $3/2^-$ resonance is well established, there is a controversy concerning the excited $1/2^-$ resonance reported in some experiments as low lying and narrow ($E_R \sim 1$ MeV, $\Gamma \leq 1$ MeV) while in others as very broad and located at a higher energy. This issue cannot be addressed by *ab initio* theoretical calculations based on traditional bound-state methods. We introduce a new unified approach to nuclear bound and continuum states based on the coupling of the no-core shell model, a bound-state technique, with the no-core shell model combined with the resonating-group method, a nuclear scattering technique. Our calculations describe the ground-state resonance in agreement with experiment and, at the same time, predict a broad $1/2^-$ resonance above 2 MeV.

DOI: [10.1103/PhysRevLett.110.022505](https://doi.org/10.1103/PhysRevLett.110.022505)

PACS numbers: 21.60.De, 24.10.Cn, 25.10.+s, 27.20.+n

Exotic nuclei are the gateway to new manifestations of nuclear matter at the boundaries of stability, where the neutron-to-proton ratios are larger or smaller than those naturally occurring on Earth. In these remote regions of the nuclear landscape, our ability to understand nuclear properties in terms of the underlying forces is put to the test. Particularly interesting in this respect are systems accessible to many-body *ab initio* calculations, such as the neutron-rich isotopes of helium and, among them, ${}^7\text{He}$. Its ground state (g.s.), characterized by spin, parity and isospin $J^\pi T = 3/2^- 3/2$, lies at 0.430(3) MeV [1,2] above the threshold of a neutron (n) plus the ${}^6\text{He}$ Borromean halo, a loosely-bound state of two neutrons and an α (${}^4\text{He}$) particle. Experimentally, excited states of ${}^7\text{He}$ are populated by means of transfer reactions that usually lead to a continuous three-body background of ${}^6\text{He}$ plus n (coming from the ${}^7\text{He}$ decay) plus a third outgoing particle. The presence of such a background is a major stumbling block and has left open questions about the low-lying spectrum of this nucleus. While there is a general consensus on the existence of a $5/2^-$ resonance centered at 3.35 MeV, which mainly decays to $\alpha + 3n$ [3], the existence and position of a low-lying $1/2^-$ state are still under discussion. In particular, many experiments [4–8] (most of which are based on one-neutron knockout reactions of a ${}^8\text{He}$ beam on a carbon target) advocate the presence of a narrow ($\Gamma \leq 1$ MeV) $1/2^-$ state at about 1 MeV while several others [9–14] do not confirm it. The occurrence of a low-lying $1/2^-$ state has also been excluded by a study on the isobaric analog states of ${}^7\text{He}$ in ${}^7\text{Li}$ [15]. According to this work, a broad $1/2^-$ resonance at ~ 3.5 MeV with a width of $\Gamma \sim 10$ MeV fits data the best. Neutron-pickup and proton-removal reactions [11,12] suggest instead a $1/2^-$ resonance at about 3 MeV with a width of $\Gamma \approx 2$ MeV.

From a theoretical standpoint, addressing the controversy surrounding the $1/2^-$ resonance of ${}^7\text{He}$ requires a unified description of structural and reaction properties that cannot be realized within traditional *ab initio* bound-state approaches such as the Green's function Monte Carlo (GFMC) method [16], the no-core shell model (NCSM) [17], or the coupled cluster method [18–20]. The complex coupled cluster method was recently applied to He isotopes, but only the g.s. of ${}^7\text{He}$ was investigated [21]. In this Letter, we address the low-lying resonances of ${}^7\text{He}$ within the no-core shell model with continuum (NCSMC), a new unified approach to nuclear bound and continuum states based on the coupling of the NCSM [17] with the no-core shell model combined with the resonating-group method (NCSM/RGM) [22–27]. The NCSM is a bound-state technique, where one performs large-scale expansions of the A -body Schrödinger wave function in terms of a complete set of harmonic oscillator (HO) basis states. The A -body square-integrable eigenstates $|A\lambda J^\pi T\rangle$ are obtained by diagonalizing the Hamiltonian matrix. The NCSM/RGM allows one to go beyond bound states and treat the continuum of resonances, scattering states, and reactions by expanding the A -body wave function over an $(A - a, a)$ binary-cluster basis in the spirit of the RGM,

$$|\Phi_{\nu r}^{J^\pi T}\rangle = [([A - a\alpha_1 I_1^{\pi_1} T_1] | a\alpha_2 I_2^{\pi_2} T_2 \rangle)^{(sT)} Y_\ell(\hat{r}_{A-a,a})]^{(J^\pi T)} \times \frac{\delta(r - r_{A-a,a})}{r r_{A-a,a}}, \quad (1)$$

in which each cluster of nucleons is described within the NCSM. Here, the unknown relative motion wave functions $\gamma_\nu(r)$ between pairs of clusters, labeled by the quantum numbers $\nu = \{A - a\alpha_1 I_1^{\pi_1} T_1; a\alpha_2 I_2^{\pi_2} T_2; s\ell\}$, are obtained by solving a set of nonlocal integral-differential coupled-channel equations [23]. Both the NCSM and NCSM/RGM

preserve translational invariance and the Pauli principle. In the latter approach, the operator $\hat{\mathcal{A}}_\nu = [(A - a)!a! / A!]^{1/2} \sum_p (-)^p P$, where P are permutations of nucleons across the two clusters and p the number of interchanges characterizing them, ensures full antisymmetrization. The NCSMC ansatz for the wave function includes both A -body square-integrable and $(A - a, a)$ binary-cluster continuous basis states, according to

$$|\Psi_A^{JT}\rangle = \sum_\lambda c_\lambda |A\lambda J^\pi T\rangle + \sum_\nu \int dr r^2 \frac{\gamma_\nu(r)}{r} \hat{\mathcal{A}}_\nu |\Phi_{\nu r}^{JT}\rangle. \quad (2)$$

The NCSM sector of the basis (eigenstates $|A\lambda J^\pi T\rangle$) provides an effective description of the short- to medium-range A -body structure, while the NCSM/RGM cluster states make the theory able to handle the scattering physics of the system. The discrete, c_λ , and the continuous, $\gamma_\nu(r)$, unknowns of the NCSMC wave functions are obtained as solutions of the following coupled equations:

$$\begin{pmatrix} H_{\text{NCSM}} & \bar{h} \\ \bar{h} & \bar{\mathcal{H}} \end{pmatrix} \begin{pmatrix} c \\ \chi \end{pmatrix} = E \begin{pmatrix} 1 & \bar{g} \\ \bar{g} & 1 \end{pmatrix} \begin{pmatrix} c \\ \chi \end{pmatrix}. \quad (3)$$

Here, $(H_{\text{NCSM}})_{\lambda\lambda'} = E_\lambda \delta_{\lambda\lambda'}$ is the diagonal matrix of the NCSM energy eigenvalues; $\bar{\mathcal{H}}_{\nu\nu'} = (\mathcal{N}^{-1/2} \mathcal{H} \mathcal{N}^{-1/2})_{\nu\nu'}$ and $\chi_\nu = (\mathcal{N}^{1/2} \gamma)_\nu$ are, respectively, the Hamiltonian kernel and relative wave functions when working with orthogonalized NCSM/RGM cluster channel states [23] [obtained from $\mathcal{N}_{\nu'\nu}(r', r) = \langle \Phi_{\nu' r'}^{JT} | \hat{\mathcal{A}}_{\nu'} \hat{\mathcal{A}}_\nu | \Phi_{\nu r}^{JT} \rangle$ and $\mathcal{H}_{\nu'\nu}(r', r) = \langle \Phi_{\nu' r'}^{JT} | \hat{\mathcal{A}}_{\nu'} \hat{H} \hat{\mathcal{A}}_\nu | \Phi_{\nu r}^{JT} \rangle$]; and $\bar{g}_{\lambda\nu}(r)$ and $\bar{h}_{\lambda\nu}(r)$ are the overlap and Hamiltonian form factors describing the coupling between the two sectors of the basis, respectively proportional to the matrix elements $\langle A\lambda J^\pi T | \hat{\mathcal{A}}_\nu | \Phi_{\nu r}^{JT} \rangle$ and $\langle A\lambda J^\pi T | \hat{H} \hat{\mathcal{A}}_\nu | \Phi_{\nu r}^{JT} \rangle$. The coupled-channel equations (3) are solved by applying the microscopic R -matrix method on a Lagrange mesh [28]. Further details will be given elsewhere [29].

In the following, we proceed to discuss the results obtained by highlighting each step of the calculation and emphasizing new achievements made possible by the NCSMC. While a complete *ab initio* calculation would, in principle, require us to work with a nuclear Hamiltonian containing both two- (NN) and three-nucleon (NNN) force components, our main concern is first to develop a theory that can address open quantum systems such as ${}^7\text{He}$. Therefore, we adopt the similarity-renormalization-group (SRG) evolved [30–33] chiral next-to-next-to-next-to-leading order ($N^3\text{LO}$) NN potential of Refs. [34,35] that provides an accurate description of the NN system and omit, for the time being, both initial and SRG-induced NNN forces. Although with such a procedure results depend on the SRG parameter Λ , we note that, for $\Lambda = 2.02 \text{ fm}^{-1}$, one obtains realistic binding energies for the lightest nuclei, e.g., ${}^4\text{He}$ and, especially important for the

TABLE I. Ground-state energies of ${}^{4,6,7}\text{He}$ in MeV. An exponential fit was employed for the extrapolations.

$E_{\text{g.s.}}$ [MeV]	${}^4\text{He}$	${}^6\text{He}$	${}^7\text{He}$
NCSM $N_{\text{max}} = 12$	-28.05	-28.63	-27.33
NCSM extrapolation	-28.22(1)	-29.25(15)	-28.27(25)
Experiment	-28.30	-29.27	-28.84

present investigation, ${}^6\text{He}$ (see Table I). Consequently, this choice of NN potential allows us to perform qualitatively and quantitatively meaningful calculations for ${}^7\text{He}$ that can be compared to experiment.

We begin by presenting NCSM calculations for ${}^6\text{He}$ and ${}^7\text{He}$ that will serve as input for the subsequent investigations of ${}^7\text{He}$. These variational calculations, depending on the number of excitations N_{max} and frequency Ω of the HO basis, converge rapidly and can be easily extrapolated. At $N_{\text{max}} = 12$ (our ${}^6,7\text{He}$ limit for technical reasons), the dependence of the ${}^6\text{He}$ g.s. energy on the HO frequency is flat in the range of $\hbar\Omega \sim 16$ – 19 MeV. We choose the lower value $\hbar\Omega = 16$ MeV for our subsequent calculations. Extrapolated g.s. energies with their error estimates and the $N_{\text{max}} = 12$ results are given in Table I, and calculated ${}^6\text{He}$ excitation energies are shown in Fig. 1. The ${}^6\text{He}$ is weakly bound with all excited states unbound. Except for the lowest 2^+ state, all ${}^6\text{He}$ excited states are either broad resonances or states in the continuum. We observe a good stability of the 2^+ state with respect to the basis size of our NCSM calculations. The higher excited states, however, drop in energy with increasing N_{max} , with the most dramatic example being the multi-particle-hole 0_3^+ state.

For ${}^7\text{He}$, the NCSM predicts the g.s. to be unbound, in agreement with experiment. However, the position of the resonance with respect to the ${}^6\text{He} + n$ threshold appears to be overestimated. Obviously, it is not clear that the *ad hoc*

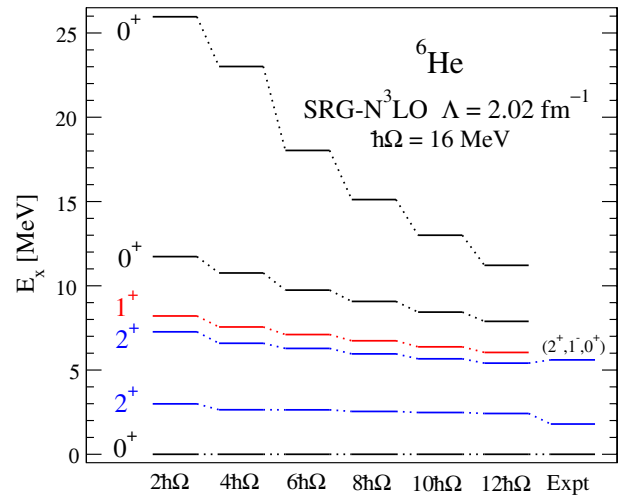


FIG. 1 (color online). Dependence of ${}^6\text{He}$ excitation energies on the size of the HO basis $N_{\text{max}} \hbar\Omega$.

TABLE II. NCSM spectroscopic factors compared to Cohen-Kurath (CK) [36] and VMC-GFMC [16,37,38] calculations and to experiment. The CK values should still be multiplied by $A/(A-1)$ to correct for the center-of-mass motion.

${}^7\text{He } J^\pi$	${}^6\text{He} - n(lj)$	NCSM	CK	VMC	GFMC	Experiment
$3/2_1^-$	$0^+ - p_{3/2}^3$	0.56	0.59	0.53	0.565	0.512(18) [2] 0.64(9) [39] 0.37(7) [11]
$3/2_1^-$	$2_1^+ - p_{1/2}^1$	0.001	0.06	0.006		
$3/2_1^-$	$2_1^+ - p_{3/2}^3$	1.97	1.15	2.02		
$3/2_1^-$	$2_2^+ - p_{1/2}^1$	0.12		0.09		
$3/2_1^-$	$2_2^+ - p_{3/2}^3$	0.42		0.30		
$1/2_1^-$	$0^+ - p_{1/2}^1$	0.94	0.69	0.91		
$1/2_1^-$	$2_1^+ - p_{3/2}^3$	0.34	0.60	0.26		
$1/2_1^-$	$2_2^+ - p_{3/2}^3$	0.93				

exponential extrapolation is valid for unbound states. In addition, no information on the width of the resonance can be obtained from this calculation performed in a square-integrable HO basis. We can, however, study the structure of the ${}^7\text{He}$ NCSM eigenstates by calculating their overlaps (related, as discussed earlier, to $\bar{g}_{\lambda\nu}$) with ${}^6\text{He} + n$ cluster states and the corresponding spectroscopic factors summarized in Table II. Overall, we find a very good agreement with the variational Monte Carlo (VMC) and GFMC results as well as with the latest experimental value for the g.s. [2]. Interesting to notice is the about equal spread of $1/2^-$ between cluster states with the ${}^6\text{He}$ in the 0^+ and 2_2^+ states. We stress that, in the present calculations, the overlap functions and spectroscopic factors are not the final products to be compared to experiment but are rather inputs to more sophisticated NCSMC calculations.

Next, we present NCSMC ${}^7\text{He}$ calculations obtained by solving Eq. (3) in a model space containing the six lowest negative-parity ($3/2_1^-$, $1/2^-$, $5/2^-$, $3/2_2^-$, $3/2_3^-$, $3/2_4^-$) and four lowest positive-parity ($1/2_1^+$, $5/2_1^+$, $3/2_2^+$, $5/2_2^+$) NCSM eigenstates of ${}^7\text{He}$ as well as $n + {}^6\text{He}$ binary-cluster states including up to the three lowest eigenstates of ${}^6\text{He}$, i.e., 0^+ , 2_1^+ , and 2_2^+ (see Fig. 1). These results are also compared to those obtained by keeping only the binary-cluster part of such a model space [corresponding to the second term in the right-hand side of Eq. (2)], i.e., by solving the coupled-channel NCSM/RGM equations $\bar{\mathcal{H}}\chi = E\chi$. First, in Fig. 2, we study the dependence of the $3/2^-$ g.s. diagonal phase shifts on the number of ${}^6\text{He}$ eigenstates included in the NCSM/RGM (blue lines) and NCSMC (red lines) calculations. The NCSM/RGM calculation with the ${}^6\text{He}$ target restricted to its g.s. does not produce a ${}^7\text{He } 3/2^-$ resonance (the phase shift does not reach 90 degrees). A ${}^2P_{3/2}$ resonance does appear once the 2_1^+ state of ${}^6\text{He}$ is coupled, and the resonance position further moves to lower energy with the inclusion of the second 2^+ state of ${}^6\text{He}$. On the contrary,

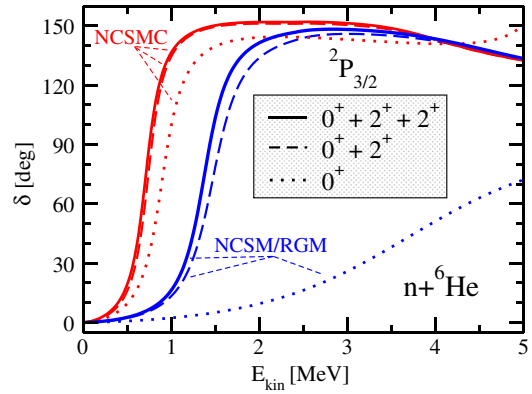


FIG. 2 (color online). Dependence of the NCSM/RGM (blue lines) and NCSMC (red lines) ${}^6\text{He} + n$ diagonal phase shifts of the ${}^7\text{He } 3/2^-$ g.s. on the number of ${}^6\text{He}$ states included in the binary-cluster basis. The short-dashed, long-dashed, and solid curves correspond to calculations with the ${}^6\text{He}$, 0^+ g.s. only; 0^+ , 2^+ states; and 0^+ , 2^+ , 2^+ states, respectively.

the ${}^2P_{3/2}$ resonance is already present in the NCSMC calculation with only the g.s. of ${}^6\text{He}$. In fact, this NCSMC model space is already enough to obtain the ${}^7\text{He } 3/2^-$ g.s. resonance at about 1 MeV above threshold, which is lower than the NCSM/RGM prediction when three ${}^6\text{He}$ states are included. Adding the 2_1^+ state of ${}^6\text{He}$ generates a modest shift of the resonance to a still lower energy, while the second 2^+ state of ${}^6\text{He}$ has no significant influence. We further observe that the resonance position in the NCSMC calculation is lower than the NCSM/RGM one by about 0.7 MeV. This difference is due to the additional correlations brought by the ${}^7\text{He}$ eigenstates that are coupled to the $n + {}^6\text{He}$ binary-cluster states in the NCSMC and that compensate for higher excited states of the ${}^6\text{He}$ target omitted in the NCSM/RGM sector of the basis. These include both positive-parity states, some of which are shown in Fig. 1, and negative-parity excitations, e.g., the 1^- soft dipole excitation, etc. While NCSM/RGM calculations with a large number of cluster excited states can become prohibitively expensive, the coupling of a few square-integrable NCSM eigenstates of the composite system is straightforward.

Panels (a) and (b) of Fig. 3 show the five P -wave and ${}^2S_{1/2}$ $n + {}^6\text{He}$ phase shifts calculated within the NCSM/RGM and NCSMC approaches, respectively. The adopted model spaces are the same as described above. As expected from a variational calculation, the introduction of the additional A -body correlations carried by the $|AAJ^\pi T\rangle$ basis states [i.e., going from (a) to (b)] lowers the centroids of all ${}^7\text{He}$ resonances. In particular, the ${}^7\text{He } 3/2^-$ g.s. and $5/2^-$ excited state are pushed toward the ${}^6\text{He} + n$ threshold, closer to their respective experimental positions.

The experimental values for the centroids of the accepted ${}^7\text{He } 3/2^-$ and $5/2^-$ resonances and the possible $1/2^-$ states are shown in Table III, together with our $N_{\max} = 12$ calculations. Within both NCSM/RGM and NCSMC,

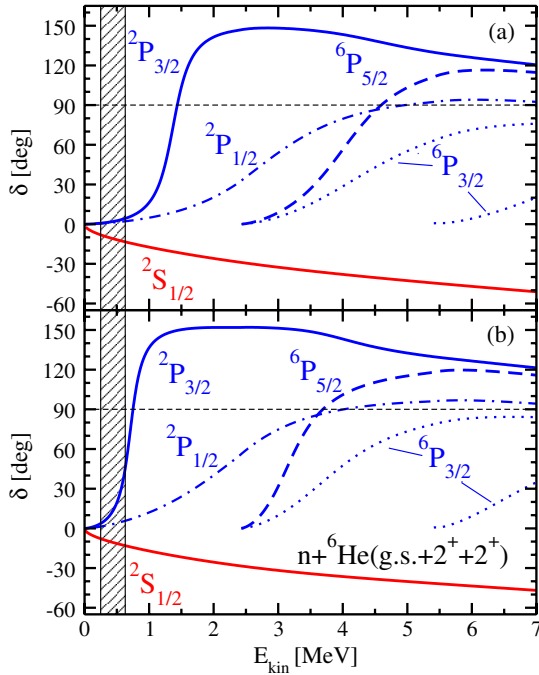


FIG. 3 (color online). (a) NCSM/RGM and (b) NCSMC ${}^6\text{He} + n$ diagonal phase shifts (except ${}^6P_{3/2}$, which are eigenphase shifts) as a function of the kinetic energy in the center of mass. The dashed vertical area centered at 0.43 MeV indicates the experimental centroid and width of the ${}^7\text{He}$ g.s. [1,2]. In all calculations, the lowest three ${}^6\text{He}$ states have been included in the binary-cluster basis. See the text for further details.

the resonance centroids E_R are obtained as the values of the kinetic energy in the center of mass E_{kin} for which the first derivative of the phase shifts is maximal [41]. The resonance widths are then computed from the phase shifts according to (see, e.g., Ref. [42])

$$\Gamma = \frac{2}{d\delta(E_{\text{kin}})/dE_{\text{kin}}} \Big|_{E_{\text{kin}}=E_R}. \quad (4)$$

An alternative, less general, choice for the resonance energy E_R could be the kinetic energy corresponding to a phase shift of $\pi/2$ (thin dashed lines in Fig. 3). At the same time, while Eq. (4) is safely applicable to sharp resonances, broad resonances would require an analysis of the scattering matrix in the complex plane. As we are more interested in

a qualitative discussion of the results, here we use the above extraction procedure for broad resonances as well. The two alternative ways of choosing E_R lead to basically identical results for the sharp $3/2^-$ resonance; however, the same is not true of the broader $5/2^-$ and the very broad $1/2^-$ resonances.

Compared to experiment, NCSMC resonance positions and widths are slightly larger in the case of the $3/2^-$ g.s. whereas they are lower for the $5/2^-$, although our determination of the width should be taken with some caution in this case. As for the $1/2^-$ resonance, the experimental situation is not clear, as discussed in the introduction and documented in Table III. While the centroid energies of Refs. [11,12,15] are comparable, the widths are very different. With the present determination of E_R and Γ , the NCSMC results are in fair agreement with the neutron-pickup and proton-removal reaction experiments [11,12] and definitely do not support the hypothesis of a low-lying ($E_R \sim 1$ MeV) narrow ($\Gamma \leq 1$ MeV) $1/2^-$ resonance [4–8]. In addition, our NCSMC calculations predict two broad ${}^6P_{3/2}$ resonances (dominated, respectively, by the first and second 2^+ states of ${}^6\text{He}$) at about 3.7 and 6.5 MeV with widths of 2.8 and 4.3 MeV, respectively. The corresponding eigenphase shifts do not reach $\pi/2$; see Fig. 3. In experiment, there is a resonance of undetermined spin and parity at 6.2(3) MeV with a width of 4(1) MeV [40]. Finally, we note that the NCSMC g.s. resonance energy, 0.71 MeV, is lower but compatible with the extrapolated NCSM value of 0.98(29) MeV (see Tables I and III).

In summary, we introduced a new unified approach to nuclear bound and continuum states based on the coupling of the no-core shell model with the no-core shell model combined with the resonating-group method and demonstrated its potentials in calculations of ${}^7\text{He}$ resonances. Our results help discriminate among three contradictory measurements concerning the nature of the $1/2^-$ resonance and, in particular, do not support the hypothesis of a low-lying and narrow $1/2^-$ resonance in ${}^7\text{He}$.

Computing support came in part from the LLNL institutional Computing Grand Challenge Program. This work was prepared in part by the LLNL under Contract No. DE-AC52-07NA27344. Support from the U.S. DOE/SC/NP (Work Proposal No. SCW1158) and the Natural Sciences and Engineering Research Council of Canada (NSERC)

TABLE III. Experimental and theoretical resonance centroids and widths in MeV for the $3/2^-$ g.s. and the $5/2^-$ and $1/2^-$ excited states of ${}^7\text{He}$. See the text for more details.

J^π	E_R	Experiment		NCSMC		NCSM/RGM		NCSM
		Γ	Reference	E_R	Γ	E_R	Γ	E_R
$3/2^-$	0.430(3)	0.182(5)	[2]	0.71	0.30	1.39	0.46	1.30
$5/2^-$	3.35(10)	1.99(17)	[40]	3.13	1.07	4.00	1.75	4.56
$1/2^-$	3.03(10)	2	[11]	2.39	2.89	2.66	3.02	3.26
	3.53	10	[15]					
	1.0(1)	0.75(8)	[5]					

Grant No. 401945-2011 is acknowledged. TRIUMF receives funding via a contribution through the National Research Council Canada. This research was supported in part by Grant No. PAI-P6-23 of the Belgian Office for Scientific Policy and by the European Union Seventh Framework Programme under Grant Agreement No. 62010.

*simone.baroni@ulb.ac.be

†navratil@triumf.ca

‡quaglioni1@lnl.gov

- [1] R.H. Stokes and P.G. Young, *Phys. Rev. Lett.* **18**, 611 (1967); *Phys. Rev.* **178**, 2024 (1969).
- [2] Z.X. Cao *et al.*, *Phys. Lett. B* **707**, 46 (2012).
- [3] A.A. Korshennikov *et al.*, *Phys. Rev. Lett.* **82**, 3581 (1999).
- [4] K. Markenroth *et al.*, *Nucl. Phys.* **A679**, 462 (2001).
- [5] M. Meister *et al.*, *Phys. Rev. Lett.* **88**, 102501 (2002).
- [6] F. Skaza *et al.*, *Phys. Rev. C* **73**, 044301 (2006).
- [7] N. Ryezayeva *et al.*, *Phys. Lett. B* **639**, 623 (2006).
- [8] V. Lapoux, N. Alamanos, and N. Keeley, *J. Phys. Conf. Ser.* **49**, 161 (2006).
- [9] H.G. Bohlen, R. Kalpakchieva, A. Blažević, B. Gebauer, T. Massey, W. von Oertzen, and S. Thummerer, *Phys. Rev. C* **64**, 024312 (2001).
- [10] G.V. Rogachev *et al.*, *Phys. Rev. Lett.* **92**, 232502 (2004).
- [11] A.H. Wuosmaa *et al.*, *Phys. Rev. C* **72**, 061301 (2005).
- [12] A.H. Wuosmaa *et al.*, *Phys. Rev. C* **78**, 041302 (2008).
- [13] D.H. Denby *et al.*, *Phys. Rev. C* **78**, 044303 (2008).
- [14] Yu. Aksyutina *et al.*, *Phys. Lett. B* **679**, 191 (2009).
- [15] P. Boutachkov *et al.*, *Phys. Rev. Lett.* **95**, 132502 (2005).
- [16] B.S. Pudliner, V.R. Pandharipande, J. Carlson, S.C. Pieper, and R.B. Wiringa, *Phys. Rev. C* **56**, 1720 (1997); R.B. Wiringa, S.C. Pieper, J. Carlson, and V.R. Pandharipande, *Phys. Rev. C* **62**, 014001 (2000); S.C. Pieper and R.B. Wiringa, *Annu. Rev. Nucl. Part. Sci.* **51**, 53 (2001); S.C. Pieper, K. Varga, and R.B. Wiringa, *Phys. Rev. C* **66**, 044310 (2002).
- [17] P. Navrátil, J.P. Vary, and B.R. Barrett, *Phys. Rev. Lett.* **84**, 5728 (2000).
- [18] G. Hagen, T. Papenbrock, D.J. Dean, and M. Hjorth-Jensen, *Phys. Rev. Lett.* **101**, 092502 (2008).
- [19] G. Hagen, M. Hjorth-Jensen, G.R. Jansen, R. Machleidt, and T. Papenbrock, *Phys. Rev. Lett.* **108**, 242501 (2012).
- [20] R. Roth, S. Binder, K. Vobig, A. Calci, J. Langhammer, and P. Navrátil, *Phys. Rev. Lett.* **109**, 052501 (2012).
- [21] G. Hagen, D.J. Dean, M. Hjorth-Jensen, and T. Papenbrock, *Phys. Lett. B* **656**, 169 (2007).
- [22] S. Quaglioni and P. Navrátil, *Phys. Rev. Lett.* **101**, 092501 (2008).
- [23] S. Quaglioni and P. Navrátil, *Phys. Rev. C* **79**, 044606 (2009).
- [24] P. Navrátil, R. Roth, and S. Quaglioni, *Phys. Rev. C* **82**, 034609 (2010).
- [25] P. Navrátil, R. Roth, and S. Quaglioni, *Phys. Lett. B* **704**, 379 (2011).
- [26] P. Navrátil and S. Quaglioni, *Phys. Rev. C* **83**, 044609 (2011).
- [27] P. Navrátil and S. Quaglioni, *Phys. Rev. Lett.* **108**, 042503 (2012).
- [28] M. Hesse, J.-M. Sparenberg, F. Van Raemdonck, and D. Baye, *Nucl. Phys.* **A640**, 37 (1998); M. Hesse, J. Roland, and D. Baye, *Nucl. Phys.* **A709**, 184 (2002).
- [29] S. Baroni, P. Navrátil, and S. Quaglioni (to be published).
- [30] S.K. Bogner, R.J. Furnstahl, and R.J. Perry, *Phys. Rev. C* **75**, 061001 (2007).
- [31] R. Roth, S. Reinhardt, and H. Hergert, *Phys. Rev. C* **77**, 064003 (2008).
- [32] R. Roth, T. Neff, and H. Feldmeier, *Prog. Part. Nucl. Phys.* **65**, 50 (2010).
- [33] S.K. Bogner, R.J. Furnstahl, and A. Schwenk, *Prog. Part. Nucl. Phys.* **65**, 94 (2010).
- [34] D.R. Entem and R. Machleidt, *Phys. Rev. C* **68**, 041001 (2003).
- [35] R. Machleidt and D.R. Entem, *Phys. Rep.* **503**, 1 (2011).
- [36] S. Cohen and D. Kurath, *Nucl. Phys.* **A73**, 1 (1965).
- [37] I. Brida, S.C. Pieper, and R.B. Wiringa, *Phys. Rev. C* **84**, 024319 (2011).
- [38] R.B. Wiringa (private communication).
- [39] F. Beck, D. Frekers, P. von Neumann-Cosel, A. Richter, N. Ryezayeva, and I.J. Thompson, *Phys. Lett. B* **645**, 128 (2007).
- [40] D.R. Tilley, C.M. Cheves, J.L. Godwin, G.M. Hale, H.M. Hofmann, J.H. Kelley, C.G. Sheu, and H.R. Weller, *Nucl. Phys.* **A708**, 3 (2002).
- [41] I.J. Thompson (private communication).
- [42] I.J. Thompson and F. Nunes, *Nuclear Reactions for Astrophysics* (Cambridge University Press, Cambridge, England, 2009), p. 301.